European Journal of Haematology

WILEY

European Journal of Haematology

ORIGINAL ARTICLE OPEN ACCESS

Microbiome-Based Modeling of CAR-T Therapy Response in Lymphoma: Insights From Shotgun Metagenomics Sequencing

Rafael Hernani[1] | Eliseo Albert[2] | Carlos Hernani-Morales[3,4] | Sheila Zúñiga[5] | Ana Benzaquén[1] | Laura González-Castillo[6] | Ester Colomer[2] | Júlia Morell[1] | José Francisco Català-Senent[5] | José Luis Piñana[1] | Estela Giménez[2] | Ariadna Pérez[1] | Juan Carlos Hernández-Boluda[1,7] | Ignacio Arroyo[1] | Marcos Rivada[1] | Teresa Barber[1] | Teresa Alemany[1] | Enric Santacatalina[1] | Pilar Rentero-Garrido[6] | María José Terol[1,7] | Rafael Díaz[8] | David Navarro[2,9] | Carlos Solano[1,7]

[1]Haematology Department, Hospital Clínico Universitario, INCLIVA Research Institute, Valencia, Spain | [2]Microbiology Department, Hospital Clínico Universitario, INCLIVA Research Institute, Valencia, Spain | [3]Quantum Spain, Universitat de València, Valencia, Spain | [4]IDAL, Electronic Engineering Department, ETSE-UV, Universitat de València, Valencia, Spain | [5]Bioinformatics Unit, INCLIVA Research Institute, Valencia, Spain | [6]Precision Medicine Unit, INCLIVA Research Institute, Valencia, Spain | [7]Department of Medicine, University of Valencia, Valencia, Spain | [8]Nuclear Medicine Department, Hospital Clínico Universitario, INCLIVA Research Institute, Valencia, Spain | [9]Department of Microbiology, University of Valencia, Valencia, Spain

Correspondence: Rafael Hernani (hernani_raf@gva.es)

Received: 25 September 2025 | **Revised:** 16 December 2025 | **Accepted:** 18 December 2025

Keywords: CAR-T (chimeric antigen receptor T-cell) | gut microbiome | machine learning | shotgun metagenomics sequencing

ABSTRACT

The interplay between the commensal microbiota and the mammalian immune system may influence the outcomes of T cell-driven cancer immunotherapies. However, clinical studies supporting microbiota-based interventions in chimeric antigen receptor T-cell (CAR-T) therapy remain scarce. This study included 30 adult patients with B-cell lymphoma treated with axicabtagene ciloleucel (axi-cel) or 4-1BB investigational product. Shotgun metagenomics sequencing (SMS) of fecal samples, collected before lymphodepletion and 1 month post infusion, enabled species-level resolution. We also trained 25 microbiome-based machine-learning (ML) models for response prediction. Neither prior "high-risk" antibiotics exposure nor alpha diversity influenced toxicity, response, or survival. However, dysbiosis was observed between 11 healthy controls and patients, particularly in those treated with axi-cel. SMS identified species associated with clinical outcomes. Increased abundance of *Alistipes senegalensis* and *Alistipes onderdonkii* correlated with lower neurotoxicity and improved survival, respectively. *Bifidobacterium longum* was associated with reduced cytokine release syndrome, whereas *Bifidobacterium adolescentis*, *Bifidobacterium bifidum*, and *Bifidobacterium breve* correlated with poorer survival. ML models demonstrated strong predictive performance, with some identifying non-responders using only six species selected by the Boruta method (*Bacteroides xylanisolvens*, *Bifidobacterium bifidum*, *Bifidobacterium breve*, *Eubacteriaceae bacterium Marseille-Q4139*, *Negativibacillus massiliensis*, and *Sellimonas intestinalis*). These findings deepen current knowledge and support prospective microbiota-based strategies in CAR-T therapy.

1 | Introduction

Chimeric antigen receptor T-cell (CAR-T) therapy has improved outcomes in relapsed/refractory (R/R) patients with hematological malignancies [1]. Despite promising data, treatment failure represents the primary cause of death within this specific patient subset [2]. As living drugs, CAR-T cells are also associated with potentially life-threatening immunological

toxicities, such as cytokine release syndrome (CRS) and neurotoxicity, commonly known as ICANS (immune effector cell-associated neurotoxicity syndrome) [3].

In recent years, preclinical and clinical studies have demonstrated the interplay between the commensal microbiota and the mammalian immune system [4], which could influence the efficacy and toxicity of T cell-driven cancer immunotherapies [5]. The most robust evidence has emerged from research in solid tumors, highlighting the association between microbiota diversity and response to checkpoint inhibitors (CPI) [6]. However, there is insufficient evidence to support the routine use of probiotics in patients receiving antitumor treatment, as certain bacterial species have also been linked to an increased risk of therapeutic failure or toxicity [7].

As an environmental and host factor, the gut microbiome could theoretically be modulated (e.g., through probiotics or selective antibiotic decontamination) to modify the outcomes after CAR-T therapy [5, 8–11]. However, there are few clinical studies providing the evidence to support microbiota-based intervention strategies [12–20]. Taking this into account, the present study aimed to advance understanding of the gut microbiome in the context of CAR-T therapy by employing shotgun metagenomics sequencing (SMS), which provides significantly greater sequencing depth. This enhanced sensitivity enables researchers to identify not only bacterial families and genera but also individual species with higher precision. Additionally, we integrated our data with publicly available datasets to train and refine microbiome-based machine-learning (ML) models for response prediction across different conditions.

2 | Methods

2.1 | Study Design

Adult patients with B-cell lymphoma receiving either commercial axicabtagene ciloleucel (axi-cel) or 4-1BB investigational product (4IP) were consecutively enrolled at Hospital Clínico Universitario de Valencia from March 2023 to June 2024. Two fecal samples were prospectively collected: before lymphodepleting chemotherapy (preLD) and 1 month after CAR-T infusion (D30). In January 2024, the protocol was amended to include a healthy control from the same family unit, based on the premise that under normal conditions the microbiota of cohabiting individuals exhibits a high degree of similarity [21], which could potentially enhance the success of a future intrafamilial fecal microbiota transplantation strategy given the suggested benefit of a closer donor–recipient microbiota distance in some enteropathies [22]. The study was approved by the institutional review board of Hospital Clínico Universitario de Valencia (reference code 2023/026). Written informed consent was obtained from all participants. All procedures in this study were conducted in accordance with the declaration of Helsinki.

2.2 | Healthy Controls

The healthy cohabiting family member voluntarily provided one fecal sample while accompanying their sick family member during the CAR-T admission period. Their medical history was taken, considering gastrointestinal disease history and medication intake, particularly the use of probiotics, gastric protectants, or antibiotics in the last month.

2.3 | Patient Management

Lymphodepleting chemotherapy consisted of cyclophosphamide (500 mg/m^2) and fludarabine (30 mg/m^2) daily for three consecutive days from days −5 to −3. Cytokine-release syndrome (CRS) and immune effector cell-associated neurotoxicity syndrome (ICANS) were graded according to American Society for Transplantation and Cellular Therapy recommendations [23] and managed following institutional guidelines [24]. Severe forms of CRS or ICANS were defined as grade 3 or higher. All patients received prophylaxis with quinolones and fluconazole in cases of neutropenia $< 500/mm^3$, or posaconazole in cases of corticosteroid or tocilizumab use, following institutional guidelines [3]. Broad-spectrum antibiotics, including meropenem, cefepime, ceftazidime, and piperacillin-tazobactam, were classified as "high-risk" antibiotics, as previously described [15].

2.4 | Definition and Endpoints

Overall response rate (ORR) was determined by the proportion of patients who achieved either partial (PR) or complete response (CR) after CAR-T infusion [25]. To train our ML models using the German/North American (GNA) dataset, we used the same definition of response (CR vs. no-CR at day 180) [15]. Progression-free survival (PFS) was defined as the time from CAR-T infusion until relapse, progression, or death from any cause. Overall survival (OS) was the time from CAR-T infusion until death from any cause. In addition to preinfusion variables, the study assessed the impact of D30 alpha diversity, CRS, ICANS, and the use of antibiotics, tocilizumab, and corticosteroids when evaluating response and survival outcomes. Similarly, CRS was considered a risk factor for ICANS.

2.5 | Fecal Sample Collection and Processing

Fecal samples were collected using a DNA stabilization buffer kit (Canvax Stool Sample Collection & Stabilization Kit), which was stored at −20°C in the Microbiology Department. Fecal microbiota composition was characterized through whole-genome SMS, as previously described [15]. Details of SMS analyses can be found in the Supporting Information.

2.6 | Bioinformatics Analysis

Low-quality reads and host-derived sequences were filtered out, and the resulting files were processed using the KneadData v0.12 tool (https://github.com/biobakery/kneaddata). Then, microbial communities (including bacteria, archaea, and eukaryotes) were profiled at the family ($n = 223$), genus ($n = 652$), and species ($n = 1140$) levels in each sample using MetaPhlAn 4. The microeco R package v1.10.0 was employed for calculating alpha and beta diversities. Differences in alpha diversity between

pre-lymphodepletion and D30 samples were assessed using the Wilcoxon signed-rank test for paired data. Comparisons of alpha and beta diversity between unpaired controls and either pre-lymphodepletion or D30 samples were performed using the Wilcoxon rank-sum test. To account for multiple comparisons, *p*-values were adjusted using the Benjamini–Hochberg procedure.

2.7 | Statistical Analysis

Chi-squared test with Yates correction was used for comparison of categorical variables, which included ORR, CRS, and ICANS. Kaplan–Meier curves were used to estimate survival probability, and univariate comparisons were made using the log-rank test. Mann–Whitney U tests were conducted to compare the relative abundances of taxa at different levels (family, genus, species) against key clinical variables. To enhance data visualization, we plotted the $\log_2$ ratio of the U statistic obtained from the Mann–Whitney U test. Only taxa with statistically significant differences were included in the figures. Statistical significance was determined by two-sided *p*-value <0.05. Multivariate analyses were not performed due to the small sample size. Statistical analyses were performed with RStudio version 3.6.0+ (The CRAN project), while ML models were conducted using Python version 3.11.0. Details of machine-learning analysis can be found in the Supporting Information (Methods and Table S1).

3 | Results

3.1 | Patient and Healthy Control Characteristics

Table 1 summarizes patient baseline characteristics. Briefly, 18 (60%) were treated with axi-cel, and 12 (40%) received 4IP. Although metabolic tumor volume was available for most patients, other surrogate markers of tumor burden, such as bulky disease, EASIX score, LDH, and ferritin levels were also included. Patient and disease characteristics were well balanced between the axi-cel and 4IP groups, except for the need for bridging therapy and subsequent disease evaluation prior to CAR-T infusion. Further details on infections and antibiotic use prior to lymphodepletion are provided in the Supporting Information.

In 11 patients (37%) a sample was obtained from a corresponding healthy cohabiting family member (spouse, $n=10$; sister, $n=1$). The median age of family members was 56 years (range: 38–75), and 64% were women. None of the family members had a history of gastrointestinal disease or recent use of antibiotics, probiotics, or gastric protectants.

3.2 | Gut Microbiome Characteristics

The median number of final reads after trimming and decontamination was 11 794 088 (range: 7 315 628–96 241 730). Of these, 78.64% (range: 50.06–90.83) were successfully classified taxonomically. The microbiome was analyzed at the family, genus, and species levels (Figure 1). PreLD and D30 alpha diversity showed no correlation with baseline patient or disease characteristics. As shown in Figure 2A, alpha diversity decreased after CAR-T infusion ($p=0.036$). Use of antibiotics, either preLD ($p=1$) or within 30 days after CAR-T infusion (aminoglycosides, $p=0.14$; antiGP antibiotics, $p=0.26$; "high-risk" antibiotics, $p=0.38$) had no impact on preLD or D30 alpha diversity, respectively. Median alpha diversity among family members was 3.6948 (range: 3.1848–4.1213), which was statistically significant compared to preLD samples ($p=0.008$) (Figure 2B). The composition of preLD fecal samples from CAR-T cell recipients differed significantly from that of healthy volunteers (Figure 2C). Dysbiosis further increased by day 30, with a more pronounced effect observed in patients treated with axi-cel.

3.3 | Safety

In total, 22 (73%) and 13 (63%) patients developed CRS and ICANS, respectively (Table S2), with grade 3 or higher CRS and ICANS occurring in 2 (7%) and 7 (23%) patients, respectively, without grade 5 events. Neither preLD alpha diversity nor the use of preLD antibiotics showed a correlation with CRS or ICANS. Additional clinical information concerning risk factors of immunotoxicities is provided in Table S3.

The fold-changes of species that were significantly different between CRS and ICANS groups are shown in Table 2 and Figure 3A,B. As the 4IP cohort did not develop ICANS, fold changes of species significantly associated with CRS, stratified by CAR-T product, are presented in Figure S1. The data concerning the fold-change of families and genera are included in Tables S4 and S5, respectively. Among other findings, we observed that a higher relative abundance of *Anaerotruncus colihominis* and *Bifidobacterium longum* was protective against CRS, while a higher relative abundance of *Alistipes senegalensis* was associated with a reduced risk of ICANS.

3.4 | Efficacy

Twenty-seven (90%) patients responded (CR, $n=24$ [80%]; PR, $n=3$ [10%]) at a median of 34 days (range: 26–98) after CAR-T infusion. The CR and PR rates were 72% and 17%, respectively, in patients treated with axi-cel, compared to 92% and 0% in those with 4IP infusion ($p=0.3$). The ORR showed no correlation with baseline patient or disease characteristics. Seven patients relapsed at a median of 95 days (range: 55–213) after achieving a response, including all three patients whose best response was PR.

The fold-changes of species that were significantly different between response groups (CR vs. no-CR at day 180) are shown in Table 2 and Figure 3C,D, with results stratified by CAR-T product presented in Figure S2. The data concerning the fold-change of families and genera are included in Tables S4 and S5, respectively.

3.4.1 | Microbiome-Based Modeling of Response Prediction

Twenty-five ML models were trained using GNA and Spanish (SPA) datasets. Initially, we trained on the GNA dataset to assess whether they could accurately predict CR180. To enable this

TABLE 1 | Patient and CAR-T therapy characteristics.

Characteristics[a]	Entire Cohort ($N=30$)	Differences between CAR-T products		
		Axi-cel ($n=18$)	4IP ($n=12$)	p
Age in years, median (range)	57 (38–78)	56 (40–78)	61 (38–75)	0.26
70 years old, no. (%)	5 (17)	2 (11)	3 (25)	0.62
Male sex, no. (%)	18 (60)	12 (67)	6 (50)	0.59
Diagnosis, no. (%)				
DLBCL	27 (90)	15 (83)	12 (100)	0.33
PMBCL	2 (7)	2 (11)	0	
FL	1 (3)	1 (6)	0	
Cell of origin, no. (%) [N/A, $n=1$][b]				
GCB	19 (66)	10 (59)	9 (75)	0.22
Non-GCB	9 (31)	7 (41)	2 (17)	
Myc rearrangement, no. (%) [N/A, $n=3$]	6 (20)	3 (17)	3 (25)	0.47
Primary refractory, no. (%)	13 (43)	8 (44)	5 (42)	1
Previous lines of therapy, median (range)	2 (1–4)	2 (1–4)	2 (1–4)	0.91
Prior autologous HSCT, no. (%)	7 (23)	5 (28)	2 (17)	0.79
Ann Arbor stage preLD, no. (%)[c]				
I–II	5 (17)	2 (11)	3 (25)	0.33
III	6 (20)	3 (17)	3 (25)	
IV	14 (47)	8 (44)	6 (50)	
IPI score preLD, no. (%)[b]				
0–1	13 (45)	7 (41)	6 (50)	0.49
2	6 (21)	4 (24)	2 (17)	
3	4 (14)	1 (6)	3 (25)	
4–5	6 (21)	5 (29)	1 (8)	
Bulky disease preLD, no. (%) [N/A, $n=1$]	3 (10)	3 (17)	0	0.38
ECOG preLD, no. (%) [N/A, $n=1$]				
0	16 (53)	8 (44)	8 (67)	0.13
1	9 (30)	5 (28)	4 (33)	
2	5 (17)	5 (28)	0	
Bridge therapy, no. (%)	19 (63)	15 (83)	4 (33)	0.02
Disease evaluation preLD, no. (%)				0.022
Disease progression	17 (57)	11 (61)	6 (50)	0.82
Stable disease	4 (13)	0	4 (33)	0.037
Partial response	4 (13)	2 (11)	2 (17)	1
Complete response	5 (17)	5 (28)	0	0.134
Metabolic tumor volume preLD in mL, median (range) [N/A, $n=1$]	40 (0–2356)	179 (0–2356)	23.5 (4.1–553)	0.33
HCT-CI score preLD, no. (%)				

(Continues)

TABLE 1 | (Continued)

Characteristics[a]	Entire Cohort ($N=30$)	Differences between CAR-T products		
		Axi-cel ($n=18$)	4IP ($n=12$)	p
0–2	9 (30)	5 (28)	4 (33)	1
≥3	21 (70)	13 (72)	8 (67)	
Lymphocytes preLD/mm^3, median (range)	775 (250–2910)	775 (370–2160)	770 (250–2910)	1
IgG preLD in mg/dL, median (range)	658 (257–1118)	649 (296–972)	661 (257–1118)	0.88
EASIX score preLD, median (range)	1.54 (0.37–9.22)	1.87 (0.49–9.22)	0.89 (0.37–3.12)	0.53
High HEMATOTOX score preLD, no. (%)	15 (50)	11 (61)	4 (33)	0.26
Ferritin preLD in ng/mL, median (range)	515 (31–35 777)	1030 (31–35 777)	278 (63–773)	0.26
Ferritin preLD > UNL, no. (%)	21 (70)	15 (83)	6 (50)	0.12
LDH preLD in U/L, median (range)	214 (124–1498)	280 (134–1498)	214 (124–373)	0.26
LDH preLD > UNL, no. (%)	15 (50)	11 (61)	4 (33)	0.26
Infections 30 days preLD, no. (%)	4 (13)	3 (17)	1 (8)	0.91
Antibiotics 30 days preLD, no. (%)	5 (17)	4 (22)	1 (8)	0.62
Antibiotics between CAR-T infusion and D30, no. (%)	30 (100)	18 (100)	12 (100)	1
"High-risk"	23 (77)	17 (94)	6 (50)	0.017
Anti-GP antibiotics	12 (40)	10 (56)	2 (17)	0.08
Aminoglycosides	13 (43)	10 (56)	3 (25)	0.2
Alpha diversity, median (range)				
PreLD	3.259 (1.47–4.06)	3.228 (1.47–3.95)	3.263 (1.94–4.06)	1
At D30 after CAR-T infusion	2.812 (1.47–3.66)	2.8875 (1.47–3.66)	2.645 (1.74–3.61)	1

Abbreviations: 4IP, 4-1BB investigational product; Anti-GP, anti-Gram-positive; Axi-cel, axicabtagene ciloleucel; CAR-T, chimeric antigen receptor T-cell; D30, day 30; DLBCL, diffuse large B-cell lymphoma; EASIX, Endothelial Activation and Stress Index; ECOG, Eastern Cooperative Oncology Group; FL, follicular lymphoma; GCB, germinal center B-cell like; HCT-CI, hematopoietic cell transplantation-specific comorbidity index; HSCT, hematopoietic stem cell transplantation; IPI, international prognostic index; N/A, not available; PMBCL, primary mediastinal large B-cell lymphoma; preLD, pre-lymphodepleting chemotherapy; U/L, units per liter; UNL, upper normal limit.
[a]Percentages may not add up to 100 because of rounding.
[b]One patient with follicular lymphoma was excluded from cellular origin and IPI data.
[c]Five (17%) patients achieved complete response after bridging at the time of lymphodepleting chemotherapy.

analysis, we first identified and selected the species common to both the GNA dataset and our own, reducing the number of species from 1140 to 920 for model training. However, the results were suboptimal, likely due to substantial differences between the datasets. The top five models, ranked by the precision of the non-response class (negative predictive value), are presented in Table S6.

Subsequently, we trained the same ML models exclusively on our dataset, which contained 1140 species across 30 patients, with both preLD and D30 samples, yielding a total of 60 samples. The primary challenge was the relatively small sample size compared to the GNA dataset. Since our goal was to predict CR180, both preLD and D30 microbial abundances were expected to have a causal relationship with the target variable. To maximize the available data, we incorporated both preLD and D30 microbial abundances for model training. Additionally, we explored different combinations of microbial species to determine an optimal subset for model training, aiming to reduce the number of species required for accurate prediction. The datasets considered included: (i) whole dataset (all species); (ii) shared dataset (920 species common to both the SPA and GNA datasets); (iii) Mann–Whitney dataset (46 species identified as statistically significant via the Mann–Whitney U test); (iv) Boruta dataset (6 species selected using the Boruta feature selection method [*Bacteroides xylanisolvens*, *Bifidobacterium bifidum*, *Bifidobacterium breve*, *Eubacteriaceae bacterium Marseille Q4139*, *Negativibacillus massiliensis*, and *Sellimonas intestinalis*]). We also performed training-test splits to assess generalization performance and mitigate overfitting, ensuring that both subsets remained statistically representative of the original dataset. Given our limited sample size, we experimented with 15% and 25% test splits. The predictive performance of different models varied according to dataset size and feature selection strategy. The top five models for each included dataset, ranked by the precision of the non-response class (negative predictive value), are presented in Table S7. We additionally evaluated sensitivity, specificity, precision (positive predictive value [PPV]), negative predictive value, and F1-scores for both classes. These

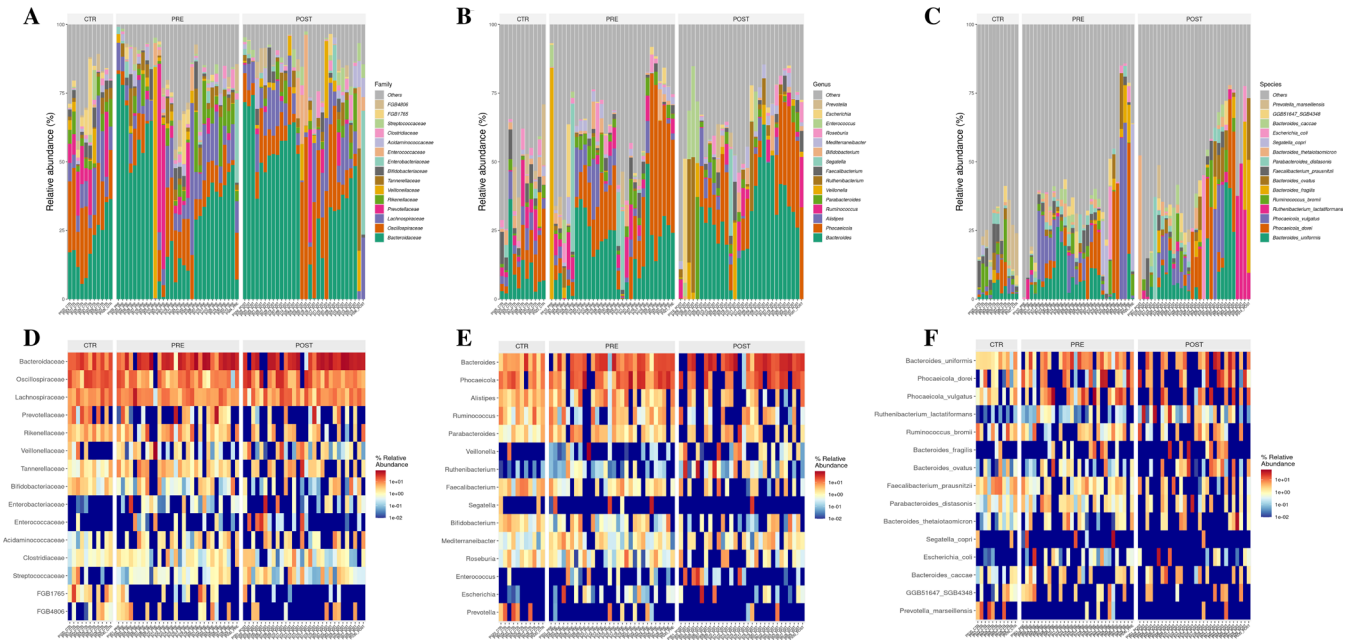

FIGURE 1 | Abundance values of the 15 most common taxa in the analyzed samples. (A) Families, (B) genera, and (C) species identified in each sample. (D) Heatmap displaying the relative abundances of the top families, (E) genera, and (F) species in each sample (relative abundance is represented by the color intensity of the cells).

metrics provided insight not only into predictive performance but also into the likelihood of false positives, as PPV and F1-score are closely related to the false discovery rate. This allowed us to quantify the reliability of predictions under class imbalance.

3.5 | Survival

Seventeen (57%) patients remained alive and progression-free at a median follow-up of 16 months (range: 10–21) after CAR-T infusion. The probability of PFS at 1 year was 56% (95% CI, 38–74) (Figure S4A). Twenty (67%) patients remained alive at a median follow-up of 15 months (range: 9–21) after CAR-T infusion, while three (10%) patients died without R/R disease at a median follow-up of 199 days (range: 296–344) after CAR-T infusion (infection, $n = 2$; solid tumor, $n = 1$). The probability of OS at 1 year was 66% (95% CI, 49–83) (Figure S4B). Neither preLD/D30 alpha diversity, antibiotic exposure (either preLD or within 30 days after CAR-T infusion), nor CAR-T product (Figure S4C,D) correlated with PFS or OS. Additional details regarding clinical prognostic factors for PFS and OS are provided in Table S8.

The fold-changes of species that were significantly different between PFS (alive and disease-free vs. dead or R/R at 12 months) and OS groups (alive vs. dead at 12 months) are shown in Table 2 and Figure 3E–H, with results stratified by CAR-T product presented in Figure S3. The data concerning the fold-change of families and genera are included in Tables S4 and S5, respectively. A higher relative abundance of *Clostridium* sp. *AM33-3*, *Coprococcus eutactus*, *Eubacteriaceae bacterium*, *Segatella copri*, *Alistipes onderdonkii*, and *Clostridium* sp. *AF36-4* was associated with better PFS. Finally, we calculated PFS curves for patients stratified by the median baseline relative abundance of species that were statistically significant in the Mann–Whitney test (Figure 4).

4 | Discussion

This study aimed to expand the limited practical knowledge of gut microbiota in the context of CAR-T therapy for R/R lymphoma. To achieve this, we employed SMS, which, although more complex and costly, offers significantly greater sequencing depth, enabling species-level resolution. Additionally, we implemented microbiome-based ML models for response prediction, leveraging previously published datasets for training.

To date, few studies have analyzed the impact of gut microbiota on CAR-T therapy for hematological malignancies. In a study by Smith et al., 16S rRNA and SMS profiling was conducted in fecal samples from 48 patients (preLD sample, $n = 26$) [13], identifying specific bacterial taxa and metabolic pathways associated with clinical outcomes. Hu et al. employed 16S rRNA analysis to investigate the gut microbiome at the genus level in 81 patients undergoing CAR-T therapy for multiple myeloma [14]. Significant temporal differences in diversity and abundance were observed between patients achieving CR and PR. Additionally, they constructed a correlation network linking gut microbes, serum cytokines, and immune cells. More recently, SMS was performed in 116 patients with R/R lymphoma across five centers in Germany and the US [15]. Fecal samples were collected at various time points ranging from day −62 to day +208. Consistent with previous studies, they identified specific bacterial taxa and metabolic pathways linked to response and survival. In our study, SMS revealed several species with an apparent influence on toxicity

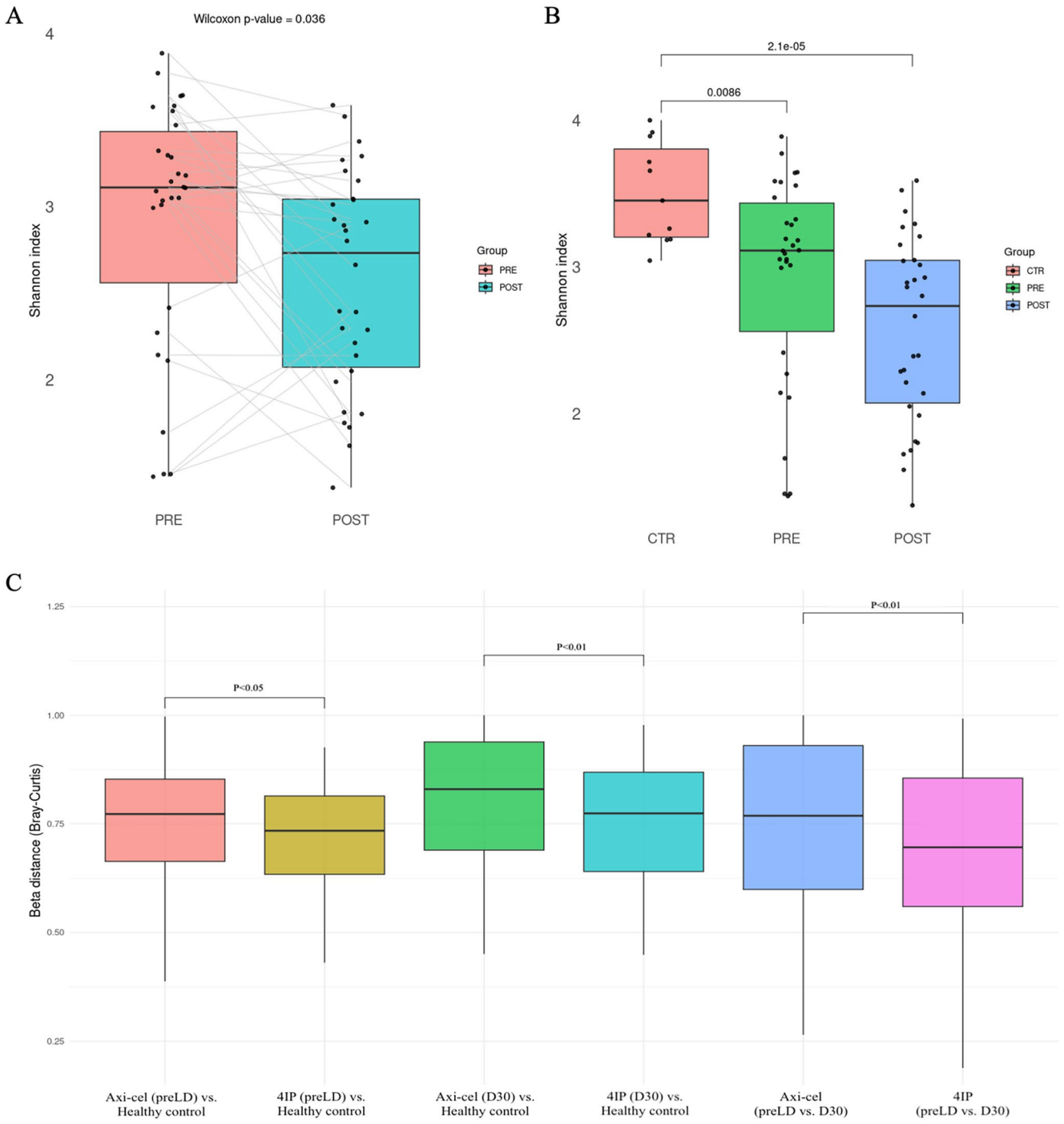

FIGURE 2 | Comparison of microbiota diversity among healthy family control, prelymphodepletion samples, and day 30 post-infusion samples. (A) Paired analysis of alpha diversity. (B) Comparison of alpha diversity between controls and patient samples. (C) Beta diversity based on the Bray–Curtis dissimilarity.

and survival outcomes. For instance, an increased abundance of *Alistipes senegalensis* and *Alistipes onderdonkii* correlated with lower ICANS incidence and improved PFS, respectively. *Alistipes* species, comprising 13 Gram-negative anaerobic bacilli, have recently been suggested to exert protective effects against various conditions, including liver fibrosis, colitis, cancer immunotherapy, and cardiovascular disease [31]. Certain species within the *Bifidobacterium* genus, a group of Gram-positive, anaerobic bacteria from the phylum *Actinomycetota*, also appeared to play a role in CAR-T outcomes. A higher abundance of *B. longum* has been associated with reduced CRS, further supporting its beneficial role in the context of immunotherapies, as it has previously been linked to response and survival in both CAR-T therapy and CPI in melanoma [15, 27]. However, increased levels of *B. adolescentis*, *B. bifidum*, and *B. breve* correlated with poorer PFS and/or OS. These findings contrast with prior data in both CAR-T therapy and CPI-treated melanoma patients [13, 27, 28].

TABLE 2 | Microbiome species associated with immunotoxicities, response, and survival outcomes after CAR-T therapy.

	CRS		ICANS		CR at 6 months		PFS at 12 months		OS at 12 months	
Species[i]	**log_2(U1/U2)**	***p***	**log2(U1/U2)**	***p***	**log2(U1/U2)**	***p***	**log2(U1/U2)**	***p***	**log2(U1/U2)**	***p***
Prelymphodepletion sample										
Alistipes_senegalensis			1.5590	0.0071						
Alistipes_sp_AF17_16					−0.6521	0.0320				
Anaerobutyricum_soehngenii	1.3536	0.0221			−1.2847	0.0234				
Anaeromassilibacillus_sp_An172	0.7370	0.0197								
Anaerotruncus_colihominis[a]	1.8365	0.0204								
Bacterium_210917_DFI_7_65					−1.0518	0.0353				
Bacteroides_eggerthii[b]					−1.0518	0.0353	−1.0196	0.0267		
Bacteroides_xylanisolvens					−2.7814	0.0008	−1.5418	0.0182		
Bifidobacterium_adolescentis[c]					−1.2115	0.0389				
Bifidobacterium_bifidum					−1.5146	0.0060	−1.3265	0.0080	−1.3270	0.0117
Bifidobacterium_breve[c,d]					−1.0000	0.0071	−0.6781	0.0445		
Bifidobacterium_longum[c,e]	1.7890	0.0231								
Bilophila_wadsworthia							−1.3426	0.0399	−1.7843	0.0132
Blautia_stercoris					−0.6521	0.0320			−0.5850	0.0473
Clostridium_sp_AM22_11AC	−1.2538	0.0400								
Clostridium_sp_AM33_3							0.8745	0.0391		
Clostridium_spiroforme	1.3740	0.0259								
Coprococcus_eutactus							1.0641	0.0211		
Enterocloster_citroniae									1.0544	0.0406

(Continues)

TABLE 2 | (Continued)

Species[i]	CRS		ICANS		CR at 6 months		PFS at 12 months		OS at 12 months	
	log_2(U1/U2)	*p*	log2(U1/U2)	*p*	log2(U1/U2)	*p*	log2(U1/U2)	*p*	log2(U1/U2)	*p*
Eubacteriaceae_bacterium							0.8745	0.0391		
Faecalibacillus_intestinalis									1.0544	0.0406
Faecalicatena_contorta					−1.1397	0.0147				
Gemella_sanguinis							−0.6781	0.0445		
GGB3001_SGB3992					−0.6521	0.0320	−0.5850	0.0473		
GGB3109_SGB4119			−1.1699	0.0068						
GGB3109_SGB4121									−1.2569	0.0392
GGB3537_SGB4727					−1.0172	0.0413				
GGB36331_SGB15121	0.7370	0.0197								
GGB3817_SGB5182			0.8745	0.0391						
GGB3819_SGB5184					−0.8981	0.0320	−0.9175	0.0177		
GGB3892_SGB5290					−0.6521	0.0320			−0.5850	0.0473
GGB4684_SGB6478					−0.6521	0.0320			−0.5850	0.0473
GGB87445_SGB15180					−1.2479	0.0081				
GGB9424_SGB14794	0.7370	0.0197								
GGB9512_SGB14909			1.0641	0.0211						
GGB9590_SGB15012					−0.6521	0.0320				
GGB9602_SGB15028			−0.9175	0.0177	−0.8314	0.0465				
GGB9608_SGB15041			−0.6781	0.0445						
GGB9641_SGB15117					−0.6521	0.0320			−0.5850	0.0473
GGB9695_SGB15210					−0.6521	0.0320			−0.5850	0.0473
GGB9708_SGB15233			−0.6781	0.0445						

(Continues)

TABLE 2 | (Continued)

	CRS		ICANS		CR at 6 months		PFS at 12 months		OS at 12 months	
Species[i]	**log_2(U1/U2)**	***p***	**log2(U1/U2)**	***p***	**log2(U1/U2)**	***p***	**log2(U1/U2)**	***p***	**log2(U1/U2)**	***p***
GGB9719_SGB53514					−0.6521	0.0320				
GGB9747_SGB15356			−0.6781	0.0445						
Hydrogenoanaerobacterium_saccharovorans									1.7028	0.0107
Lachnotalea_sp_AF33_28					−0.6521	0.0319			−0.5850	0.0472
Limosilactobacillus_vaginalis			−0.6781	0.0445						
Neglectibacter_timonensis					−0.6521	0.0320			−0.5850	0.0473
Parabacteroides_johnsonii	−1.5850	0.0182								
Parasutterella_excrementihominis					−0.6521	0.0320				
Parasutterella_secunda					−0.6521	0.0320			−0.5850	0.0473
Rothia_SGB49305			−0.6781	0.0445	−1.0000	0.0071	−0.6781	0.0445		
Segatella_copri							0.8745	0.0391		
Sellimonas_intestinalis					−1.8972	0.0069				
Streptococcus_anginosus			−0.9031	0.0481						
Streptococcus_gallolyticus			−0.6781	0.0445						
Streptococcus_infantis					−0.6521	0.0320				
Streptococcus_mitis			−1.1242	0.0295						
Yanshouia_hominis					−0.6521	0.0320			−0.5850	0.0473
Yeguia_hominis					−0.6521	0.0320			−0.5850	0.0473
Day 30 sample										
Alistipes_onderdonkii							1.0196	0.0467		

(Continues)

TABLE 2 | (Continued)

Species[i]	CRS		ICANS		CR at 6 months		PFS at 12 months		OS at 12 months	
	log_2(U1/U2)	*p*	log2(U1/U2)	*p*	log2(U1/U2)	*p*	log2(U1/U2)	*p*	log2(U1/U2)	*p*
Anaerofilum_sp_An201					−0.6521	0.0320				
Anaerosporobacter_mobilis									−0.5850	0.0473
Bacteroides_eggerthii[f]					−0.8646	0.0387				
Bacteroides_thetaiotaomicronc[c,g]									1.1882	0.0499
Clostridiales_bacterium_CHKCI006					−0.6521	0.0320			−0.5850	0.0473
Clostridium_porci					−1.0172	0.0413				
Clostridium_sp_AF36_4							1.0641	0.0211		
Dysosmobacter_SGB15077							−0.6781	0.0445		
Enterocloster_lavalensis									1.0544	0.0406
Eubacteriaceae_bacterium_Marseille_Q4139					−0.8981	0.0320				
GGB3057_SGB4059					−0.6521	0.0320				
GGB3109_SGB4119					−0.8981	0.0320				
GGB33469_SGB15236					−0.6521	0.0320			−0.5850	0.0473
GGB3678_SGB4991					−0.6521	0.0320				
GGB9480_SGB14875					−0.6521	0.0320			−0.5850	0.0473
GGB9602_SGB15028					−0.6521	0.0320			−0.5850	0.0473
GGB9646_SGB15123					−0.6521	0.0320			−0.5850	0.0473
Lachnoclostridium_sp_An131					−0.8314	0.0465				

(Continues)

TABLE 2 | (Continued)

	CRS		ICANS		CR at 6 months		PFS at 12 months		OS at 12 months	
Species[i]	**log_2(U1/U2)**	***p***	**log2(U1/U2)**	***p***	**log2(U1/U2)**	***p***	**log2(U1/U2)**	***p***	**log2(U1/U2)**	***p***
Limosilactobacillus_fermentum									−0.5850	0.0473
Limosilactobacillus_portuensis									−0.5850	0.0473
Mediterraneibacter_faecis					−0.6521	0.0320			−0.5850	0.0473
Oscillibacter_sp_MSJ_31					−0.6521	0.0320			−0.5850	0.0473
Parabacteroides_distasonis[a,h]									1.3270	0.0457
Parasutterella_excrementihominis					−0.6521	0.0320				
Scardovia_wiggsiae									−0.5850	0.0473
Schaalia_SGB17154									−0.5850	0.0473
TM7_phylum_sp_oral_taxon_352									−0.5850	0.0473
Tyzzerella_sp_An114									−0.5850	0.0473
Tyzzerella_sp_An114					−0.6521	0.0320				
Youxingia_wuxianensis					−0.8646	0.0387				
TM7_phylum_sp_oral_taxon_352									−0.5850	0.0473

Abbreviations: CAR-T, chimeric antigen receptor T-cell; CR, complete response; CRP, C-reactive protein; CRS, cytokine release syndrome; ICANS, immune effector cell-associated neurotoxicity syndrome; ICIs, immune checkpoint inhibitor; IL, interleukin; LDC, lymphodepletion chemotherapy; OS, overall survival; PFS, progression-free survival.

[a]Better PFS with ICIs in murine models of sarcoma and melanoma [26].

[b]A trend toward reduced systemic inflammation, as assessed by serum CRP or IL-6 levels during LDC in CAR-T patients [15].

[c]Better response to ICIs in melanoma [27–29].

[d]Better 3-month response in CAR-T patients [13].

[e]Better 6-month PFS and OS in CAR-T patients [15].

[f]Better 6-month response in CAR-T patients [15].

[g]Worse 6-month response in CAR-T patients [15].

[h]Better response to ICIs in non-small cell lung cancer models [30].

[i]Color legend: green indicates a favorable outcome (lower risk of CRS and ICANS; better prognosis for CR, PFS, and OS).

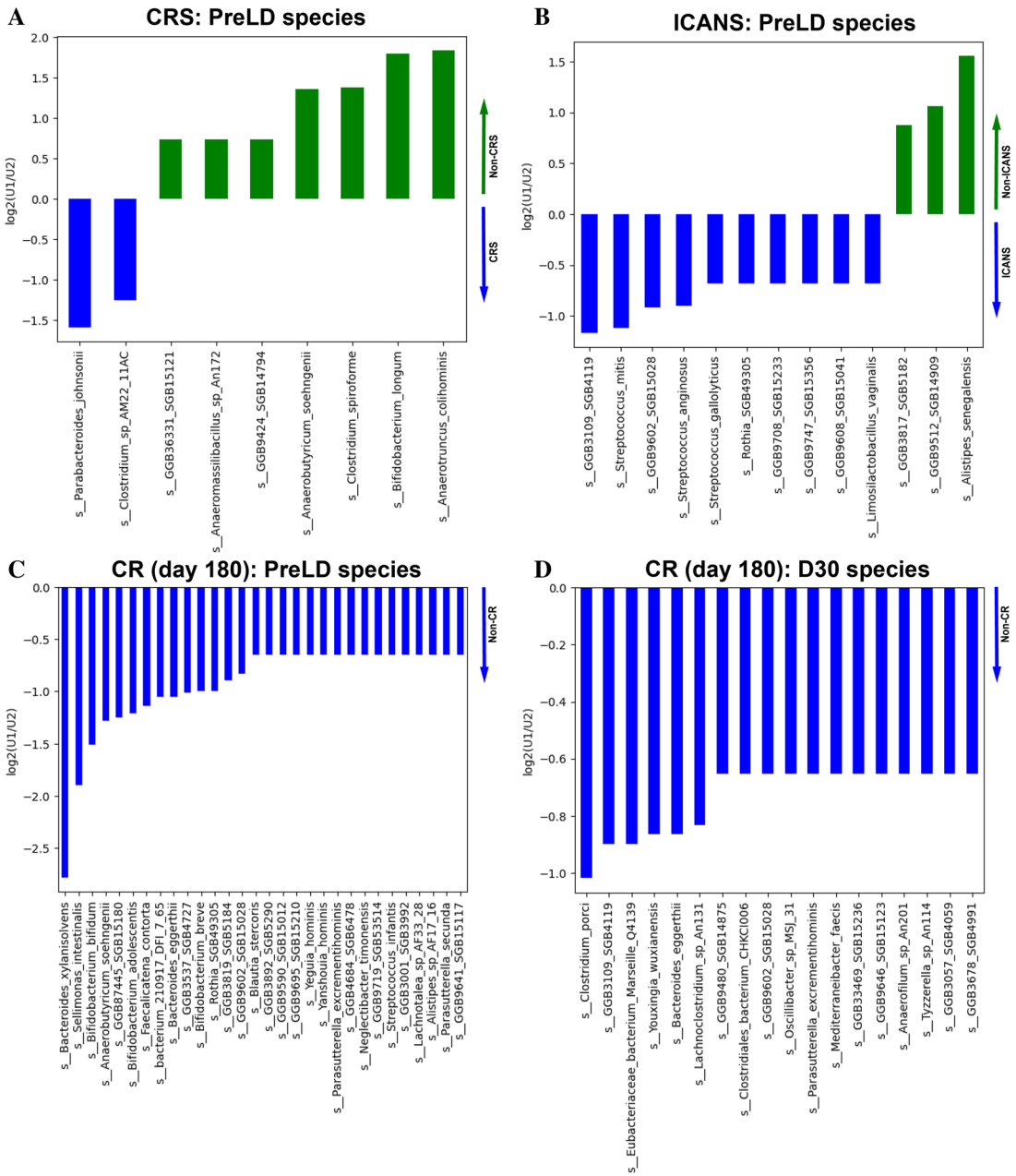

FIGURE 3 | Bar-plot showing the fold-change of species that were significantly different between groups. (A) CRS. (B) ICANS. (C and D) Response (CR vs. no-CR at day 180) according to preLD and D30 samples, respectively. (E and F) Progression-free survival (alive and disease-free vs. dead or R/R at 12 months) according to preLD and D30 samples, respectively. (G and H) Overall survival (alive vs. dead at 12 months) according to preLD and D30 samples, respectively.

Interestingly, prior antibiotic exposure showed no impact on toxicity, response, or survival in our study, contrasting with current data [13, 15, 18, 20]. This could be attributed to the small sample size; however, recent studies suggest that only prolonged post-infusion use (> 10 days) of broad-spectrum antibiotics may negatively impact survival [32]. In line with published data, we observed substantial variability in alpha diversity between healthy family controls and patients, with a significant reduction in microbial diversity, particularly after CAR-T infusion. Notably, we found no correlation between alpha diversity and baseline patient or disease characteristics, nor with antibiotic use. Moreover, we did not identify significant associations between alpha diversity and toxicity or clinical outcomes following CAR-T infusion, echoing the findings of previous studies [15, 16], but in contrast with other reports in the literature [12–14, 18]. Regarding microbiome composition, assessed by beta diversity, we found a significant dysbiosis between healthy controls and patients, particularly among those treated with axi-cel. Multiple factors could contribute to this dysbiosis, including the higher proportion of axi-cel patients requiring bridging therapies or antibiotics, which may alter microbiota composition.

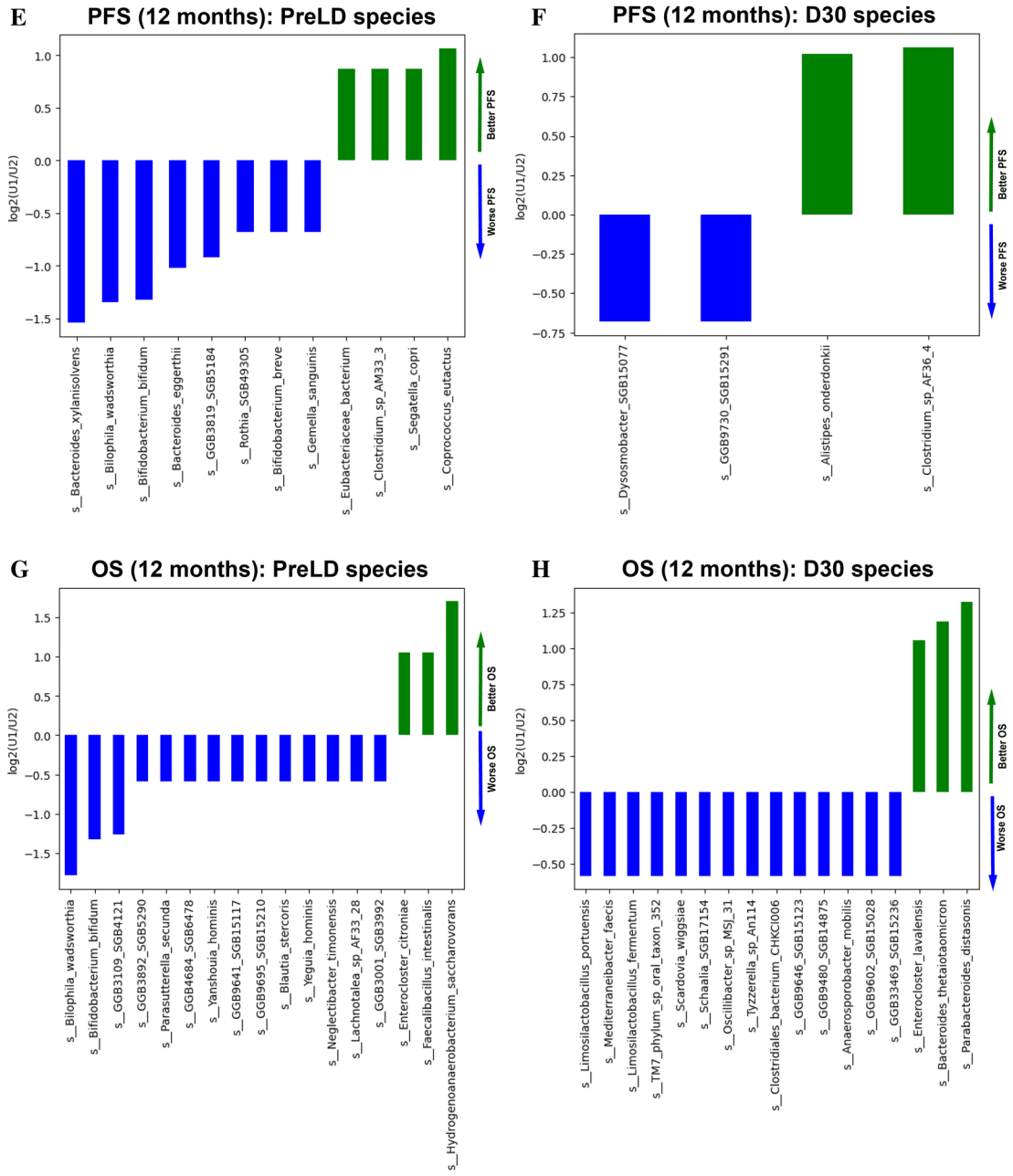

FIGURE 3 | (Continued)

Lastly, we applied ML algorithms for response prediction, with a particular focus on identifying non-responders, a subset with very poor prognosis in whom early intervention could be crucial to anticipate R/R [33]. Initially, we trained our models on the publicly available GNA dataset [15], which yielded suboptimal results, likely due to substantial disparities between datasets that could lead to differences in microbiota composition (e.g., dietary variations or different antibiotic protocols). The small sample size of our cohort may also have influenced these results [34]. Subsequently, we trained the same ML models exclusively on our dataset. Among the feature selection methods we chose was the Boruta method, a widely used approach that leverages Random Forest models to rank feature importance [35]. We selected only the most relevant variables to improve model accuracy, comprising just six species out of 1140 possible candidates in our study. If confirmed in a larger patient cohort, this approach could improve the logistical and economic feasibility of using fecal sample analysis in the context of CAR-T therapy by allowing researchers to focus exclusively on a few key species associated with clinical outcomes. Unlike previous studies that employed logistic regression or Bayesian logistic regression models trained on microbial data, sex, and age, which can provide classification probabilities and perform well if the data is sufficiently linearly separable [13, 15], our study trained 25 models exclusively on microbial data, primarily due to the small sample size. Nonetheless, logistic regression, along with LinearSVC, also emerged as one of the top-performing classifiers, suggesting that our data is also mostly linearly separable.

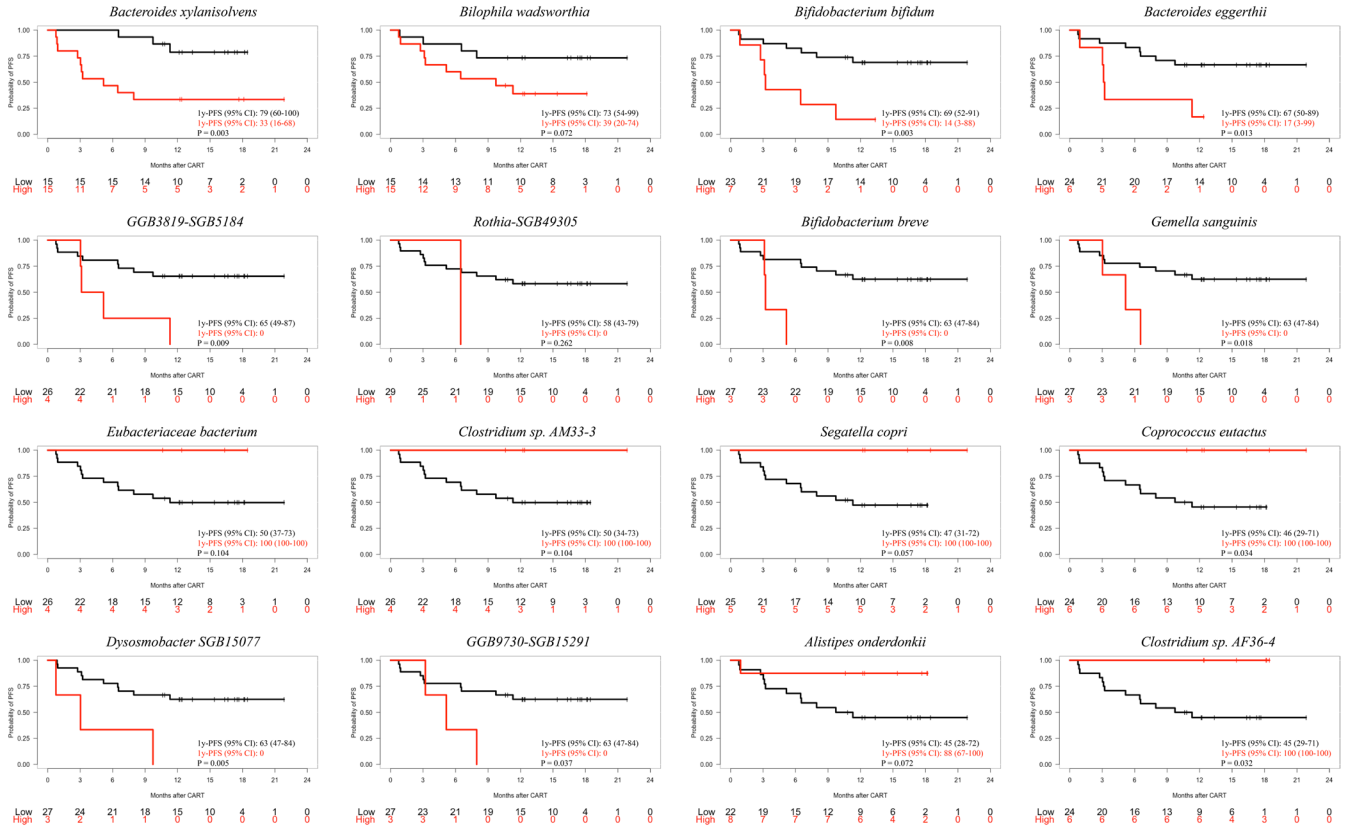

FIGURE 4 | PFS curves for patients stratified by the median baseline relative abundance of species that were statistically significant in the Mann–Whitney test.

The results of our study should be interpreted within the context of certain limitations, primarily the small sample size, driven in part by limited funding, which precluded multivariate analysis and required us to limit the test set to 15%–25%. To mitigate the risk of false discoveries, we prioritized dimensionality reduction, used robust feature selection, and reported FDR (false discovery rate)-related performance metrics such as PPV and F1-score. While these measures improve internal validity, independent validation remains essential. Despite these constraints, our study expands the limited knowledge of the microbiota in the context of CAR-T therapy by employing SMS across all samples and applying a broad range of ML models for response prediction. Altogether, the data reported herein provide a basis for prospective microbiota-based intervention strategies [36], as already implemented in other settings, such as allogeneic transplantation [37]. Given the complexity of microbiota studies and the numerous factors influencing microbial composition, international collaboration and publicly available datasets are crucial for advancing this field. Considering the potential clinical significance of these findings, well-powered, prospective studies are warranted to validate our results.

Author Contributions

R.H. conceived the paper and interpreted the data. S.Z. and J.F.C.-S. performed the bioinformatics analysis. R.H. and C.H.-M. performed the statistical analyses. All authors contributed to the writing and/or review of the manuscript and approved the final draft.

Acknowledgments

First and foremost, we would like to express our gratitude to the patients and their families for their participation in the study. We also extend our thanks to all the individuals who contributed, to varying degrees, to the collection and storage of samples, including nurses, nursing assistants, and laboratory technicians. Finally, we are especially grateful to Cristina Romero, secretary of the blood bank, for preparing the sample collection kits for patients and their families.

Funding

The Precision Medicine Unit of INCLIVA was supported by a donation from *Fundación FERO* and the Fundación para la *Promoción de Acciones Solidarias*. Illumina equipment is co-financed by the European Union through the Operational Program of the European Regional Development Fund (ERDF) of the Valencian Community 2014–2020. José Francisco Catalá-Senent was funded through a bioinformatics technician grant (CA23/00007) from the 2023 Strategic Action in Health (AES2023) call, supported by the Instituto de Salud Carlos III (ISCIII) and co-funded by the European Union.

Disclosure

The authors have nothing to report.

Ethics Statement

This study was conducted in compliance with the Declaration of Helsinki and with the approval of the local institutional review board.

Consent

All patients provided written informed consent prior to any study-related procedures.

Conflicts of Interest

The authors declare no conflicts of interest.

Data Availability Statement

The data that support the findings of this study are available from the corresponding author upon reasonable request.

References

1. A. Mitra, A. Barua, L. Huang, S. Ganguly, Q. Feng, and B. He, "From Bench to Bedside: The History and Progress of CAR T Cell Therapy," *Frontiers in Immunology* 14 (2023): 1188049.

2. M. D. Jain, J. Y. Spiegel, L. J. Nastoupil, et al., "Five-Year Follow-Up of Standard-Of-Care Axicabtagene Ciloleucel for Large B-Cell Lymphoma: Results From the US Lymphoma CAR T Consortium," *Journal of Clinical Oncology: Official Journal of the American Society of Clinical Oncology* 42, no. 30 (2024): 3581–3592.

3. R. Hernani, A. Benzaquén, and C. Solano, "Toxicities Following CAR-T Therapy for Hematological Malignancies," *Cancer Treatment Reviews* 111 (2022): 102479.

4. D. Zheng, T. Liwinski, and E. Elinav, "Interaction Between Microbiota and Immunity in Health and Disease," *Cell Research* 30, no. 6 (2020): 492–506, https://doi.org/10.1038/s41422-020-0332-7.

5. M. B. Abid, N. N. Shah, T. C. Maatman, and P. N. Hari, "Gut Microbiome and CAR-T Therapy," *Experimental Hematology & Oncology* 8 (2019): 31.

6. F. S. Gazzaniga and D. L. Kasper, "The Gut Microbiome and Cancer Response to Immune Checkpoint Inhibitors," *Journal of Clinical Investigation* 135, no. 3 (2025): e184321.

7. C. N. Spencer, J. L. McQuade, V. Gopalakrishnan, et al., "Dietary Fiber and Probiotics Influence the Gut Microbiome and Melanoma Immunotherapy Response," *Science* 374, no. 6575 (2021): 1632–1640.

8. M.-L. Schubert, R. Rohrbach, M. Schmitt, and C. K. Stein-Thoeringer, "The Potential Role of the Intestinal Micromilieu and Individual Microbes in the Immunobiology of Chimeric Antigen Receptor T-Cell Therapy," *Frontiers in Immunology* 12 (2021): 670286.

9. F. Malard, B. Gaugler, and M. Mohty, "Faecal Microbiota Transplantation in Patients With Haematological Malignancies Undergoing Cellular Therapies: From Translational Research to Routine Clinical Practice," *Lancet Haematology* 9, no. 10 (2022): e776–e785.

10. S. Asokan, N. Cullin, C. K. Stein-Thoeringer, and E. Elinav, "CAR-T Cell Therapy and the Gut Microbiota," *Cancers (Basel)* 15, no. 3 (2023): 794.

11. P.-F. Zhang and D. Xie, "Targeting the Gut Microbiota to Enhance the Antitumor Efficacy and Attenuate the Toxicity of CAR-T Cell Therapy: A New Hope?," *Frontiers in Immunology* 15 (2024): 1362133.

12. V. Blumenberg, M.-L. Schubert, E. Zamir, et al., "Antibiotic Therapy and Low Gut Microbiome Diversity Is Associated With Decreased Response and High Toxicity in BCP-ALL and DLBCL Patients After Treatment With CD19. CAR T-Cells," *Blood* 136, no. 1 (2020): 33–34, https://doi.org/10.1182/blood-2020-141210.

13. M. Smith, A. Dai, G. Ghilardi, et al., "Gut Microbiome Correlates of Response and Toxicity Following Anti-CD19 CAR T Cell Therapy," *Nature Medicine* 28, no. 4 (2022): 713–723.

14. Y. Hu, J. Li, F. Ni, et al., "CAR-T Cell Therapy-Related Cytokine Release Syndrome and Therapeutic Response Is Modulated by the Gut Microbiome in Hematologic Malignancies," *Nature Communications* 13, no. 1 (2022): 5313.

15. C. K. Stein-Thoeringer, N. Y. Saini, E. Zamir, et al., "A Non-Antibiotic-Disrupted Gut Microbiome Is Associated With Clinical Responses to CD19-CAR-T Cell Cancer Immunotherapy," *Nature Medicine* 29, no. 4 (2023): 906–916, https://doi.org/10.1038/s41591-023-02234-6.

16. Z. O'Connor, A. Bui, L. Coughlin, et al., "The Role of Gut Microbiota in Modulating Efficacy and Adverse Effects of CAR T-Cell Therapy in the Pediatric Population," *Blood* 144, no. 1 (2024): 3429, https://doi.org/10.1182/blood-2024-211415.

17. S. J. Kim, S. Yoon, W. Kang, et al., "Gut Microbiome Composition as a Prognostic Marker in CD19-Targeting CAR T-Cell Therapy for Relapsed/Refractory Diffuse Large B-Cell Lymphoma," *Blood* 144 (2024): 1595.

18. R. Garcia-Vicente, A. Rodríguez García, R. Ancos-Pintado, et al., "Enhancing CAR-T Cell Therapy for Non-Hodgkin Lymphoma Through Gut Microbiota and Butyrate," *Blood* 144 (2024): 3414.

19. N. Deschl, V. Blumenberg, M.-L. Schubert, et al., "Characterizing Environmental Adaption and Virulence of Gut Microbiome Enterococcus Spp. From Patients Receiving CD19-Targeted CAR-T Cell Therapy," *Blood* 144, no. Supplement 1 (2024): 3415–3415, https://doi.org/10.1182/blood-2024-205390.

20. R. Prasad, A. Rehman, L. Rehman, et al., "Antibiotic-Induced Loss of Gut Microbiome Metabolic Output Correlates With Clinical Responses to CAR T-Cell Therapy," *Blood* 145, no. 8 (2025): 823–839, https://doi.org/10.1182/blood.2024025366.

21. S. J. Song, C. Lauber, E. K. Costello, et al., "Cohabiting Family Members Share Microbiota With One Another and With Their Dogs," *eLife* 2 (2013): e00458.

22. R. He, P. Li, J. Wang, B. Cui, F. Zhang, and F. Zhao, "The Interplay of Gut Microbiota Between Donors and Recipients Determines the Efficacy of Fecal Microbiota Transplantation," *Gut Microbes* 14, no. 1 (2022): 2100197.

23. D. W. Lee, B. D. Santomasso, F. L. Locke, et al., "ASTCT Consensus Grading for Cytokine Release Syndrome and Neurologic Toxicity Associated With Immune Effector Cells," *Biology of Blood and Marrow Transplantation* 25, no. 4 (2019): 625–638.

24. R. Hernani, M. Aiko, R. Victorio, et al., "EEG Before Chimeric Antigen Receptor T-Cell Therapy and Early After Onset of Immune Effector Cell-Associated Neurotoxicity Syndrome," *Clinical Neurophysiology* 163 (2024): 132–142.

25. B. D. Cheson, R. I. Fisher, S. F. Barrington, et al., "Recommendations for Initial Evaluation, Staging, and Response Assessment of Hodgkin and Non-Hodgkin Lymphoma: The Lugano Classification," *Journal of Clinical Oncology* 32, no. 27 (2014): 3059–3068.

26. B. Routy, E. Le Chatelier, L. Derosa, et al., "Gut Microbiome Influences Efficacy of PD-1-Based Immunotherapy Against Epithelial Tumors," *Science* 359, no. 6371 (2018): 91–97.

27. A. Sivan, L. Corrales, N. Hubert, et al., "Commensal Bifidobacterium Promotes Antitumor Immunity and Facilitates Anti-PD-L1 Efficacy," *Science* 350, no. 6264 (2015): 1084–1089.

28. V. Matson, J. Fessler, R. Bao, et al., "The Commensal Microbiome Is Associated With Anti-PD-1 Efficacy in Metastatic Melanoma Patients," *Science* 359, no. 6371 (2018): 104–108.

29. M. Vétizou, J. M. Pitt, R. Daillère, et al., "Anticancer Immunotherapy by CTLA-4 Blockade Relies on the Gut Microbiota," *Science* 350, no. 6264 (2015): 1079–1084.

30. J. Huang, D. Liu, Y. Wang, et al., "Ginseng Polysaccharides Alter the Gut Microbiota and Kynurenine/Tryptophan Ratio, Potentiating the Antitumour Effect of Antiprogrammed Cell Death 1/Programmed Cell Death Ligand 1 (Anti-PD-1/PD-L1) Immunotherapy," *Gut* 71, no. 4 (2022): 734–745.

31. B. J. Parker, P. A. Wearsch, A. C. M. Veloo, and A. Rodriguez-Palacios, "The Genus Alistipes: Gut Bacteria With Emerging Implications to Inflammation, Cancer, and Mental Health," *Frontiers in Immunology* 11 (2020): 906.

32. R. Shouval, T. Fei, G. Gabrielli, et al., "Impact of Broad-Spectrum Antibiotic Exposure on CAR-T Therapy Outcomes in B-Cell Lymphoma: A Multicenter International Study," *Blood* 144, no. Supplement 1 (2024): 1746, https://doi.org/10.1182/blood-2024-203871.

33. G. Iacoboni, J. Iraola-Truchuelo, M. O'Reilly, et al., "Treatment Outcomes in Patients With Large B-Cell Lymphoma After Progression to Chimeric Antigen Receptor T-Cell Therapy," *HemaSphere* 8, no. 5 (2024): e62.

34. G. Infante, R. Miceli, and F. Ambrogi, "Sample Size and Predictive Performance of Machine Learning Methods With Survival Data: A Simulation Study," *Statistics in Medicine* 42, no. 30 (2023): 5657–5675.

35. M. B. Kursa and W. R. Rudnicki, "Feature Selection With the Boruta Package," *Journal of Statistical Software* 36, no. 11 (2010): 1–13.

36. K. Sandhu, X. Qi, S. Mokhtari, et al., "Trial-In-Progress: A Phase 2 Randomized Trial of Remodeling Intestinal Microbiota Using Fecal Microbiome Transplant (FMT) Among Recipients of Chimeric Antigen Receptor T Cells (CAR T)," *Blood* 146, no. Supplement 1 (2025): 5507, https://doi.org/10.1182/blood-2025-5507.

37. F. Malard, M. Labopin, E. Holler, J. Doré, E. Plantamura, and M. Mohty, "A Multicentre, Randomized, Double-Blinded, Phase 2b Study Evaluating the Efficacy and Safety of MaaT033, an Oral, Pooled Microbiome Ecosystem Therapy in Patients Undergoing Allogenic Hematopoietic Cell Transplantation to Improve Overall Survival: The Phoe," *Blood* 142, no. Suppl 1 (2023): 4947, https://doi.org/10.1182/blood-2023-185639.

Supporting Information

Additional supporting information can be found online in the Supporting Information section. **Data S1:** Supporting Information.